Journal of Applied Mechanics and Technical Physics, Vol. 41, No. 6, 2000

LOCALIZED COHERENT STRUCTURES IN THE BOUNDARY LAYER

I. G. Dodonov, V. A. Zharov, and Yu. I. Khlopkov

UDC 532.517.4:533.9

A Blasius laminar boundary layer and a steady turbulent boundary layer on a flat plate in an incompressible fluid are considered. The spectral characteristics of the Tollmien–Schlichting (TS) and Squire waves are numerically determined in a wide range of Reynolds numbers. Based on the spectral characteristics, relations determining the three-wave resonance of TS waves are studied. It is shown that the three-wave resonance is responsible for the appearance of a continuous low-frequency spectrum in the laminar region of the boundary layer. The spectral characteristics allow one to obtain quantities that enter the equations of dynamics of localized perturbations. By analogy with the laminar boundary layer, the three-wave resonance of TS waves in a turbulent boundary layer is considered.

Introduction. Based on a large amount of experimental data, physical processes in laminar and turbulent boundary layers were analyzed in [1–4]; special attention was paid to coherent structures, which may be related to the linear and nonlinear dynamics of wave packets. To describe the wave packets, one has to use the Navier–Stokes equations in the laminar boundary layer and the Reynolds equations and equations for oscillations in the turbulent boundary layer. Following [5], these equations can be represented in the form of a system of inhomogeneous Orr–Sommerfeld and Squire equations equivalent to the initial problem. Methods of identification of the special features of these flows were proposed in [6–8] for obtaining simpler equations. A number of assumptions were used: isotropy of the phase velocity, linearity of the phase velocity in terms of the absolute value of the wave vector $\boldsymbol{k}$, finiteness of the imaginary part of the frequency of TS waves with the streamwise wavenumber tending to zero, and nonmonotonic dependence of the phase velocity on $\boldsymbol{k}$.

In the case of a laminar boundary layer, the equations reduce to a system of Schrödinger nonlinear equations with respect to the envelopes of the wave packets $\tilde{\psi}_j^{(n)}$ related by harmonic and three-wave resonances, which are supplemented by a nonlinear integrodifferential equation with respect to the amplitude $\psi^{(0)}$ of the wave packet concentrated near the origin of the space of wavenumbers [6]. In the case of zero amplitude $\tilde{\psi}_j^{(n)}$, the equation for $\psi^{(0)}$ retains its own significance and has the form

$$\frac{\partial}{\partial t}\,\psi^{(0)}(t,\boldsymbol{r}_1) - \varepsilon(\bar{X}_0 - a(\bar{X}_0))\,\frac{\partial}{\partial x_1}\,\psi^{(0)}(t,\boldsymbol{r}_1) = \varepsilon^2 I^{(0)},$$

$$I^{(0)} = -b(\bar{X}_0)\int \frac{1}{|\boldsymbol{r}_1 - \boldsymbol{s}|}\,\frac{\partial}{\partial \xi}\Big(\frac{\partial^2}{\partial \xi^2} + \frac{\partial^2}{\partial \eta^2}\Big)\psi^{(0)}(t,\boldsymbol{s})\,d\boldsymbol{s}$$

$$- ix_1\,\frac{\partial a(\bar{X}_0)}{\partial \bar{X}_0}\,\frac{\partial}{\partial x_1}\,\psi^{(0)}(t,\boldsymbol{r}_1) + (d(\bar{X}_0) + Q(0))\psi^{(0)}(t,\boldsymbol{r}_1) + H_{0,0}(\tilde{\psi}^{(0)}(t,\boldsymbol{r}_1)),$$

Moscow Physicotechnical Institute, Zhukovskii 140160. Translated from Prikladnaya Mekhanika i Tekhnicheskaya Fizika, Vol. 41, No. 6, pp. 60–67, November–December, 2000. Original article submitted July 7, 1999; revision submitted September 30, 1999.

where $\boldsymbol{r}_1 = \boldsymbol{r}/\varepsilon$, $\boldsymbol{r} = (x, z)$, $\boldsymbol{r}_1 = (x_1, z_1)$, $\varepsilon^2 = (\nu\tilde{\omega}_{\max}/u_\infty^2)^{1/2}$, ν is the kinematic viscosity, u_∞ is the free-stream velocity, $\tilde{\omega}_{\max} = \max\limits_{\boldsymbol{k}} \operatorname{Imag}[\omega(\boldsymbol{k})]$, and ω is the eigenfrequency of the unstable mode of the Orr–Sommerfeld equation. The equation for $\psi^{(0)}$ contains the quantities $a(\bar{X}_0)$, $b(\bar{X}_0)$, and $d(\bar{X}_0)$ determined by the dispersion characteristic of the unstable mode of TS waves; $Q(0)$ and $H_{0,0}$ are expressed in terms of the quadratures of combinations of the eigenfunctions of the solutions of the spectral problems for the Orr–Sommerfeld and Squire equations [6] (they are considered below in more detail), and $\bar{X}_0$ is the coordinate of the "center of mass" of the wave packet normalized to the length scale $L = u_\infty/\tilde{\omega}_{\max}$. The finiteness of these parameters would indicate the applicability of this model for the description of a set of phenomena, at least weakly linear ones.

In the case of a turbulent boundary layer, we consider models based on the kinetic equation for elementary waves in the three-wave resonance approximation. The coefficients of this equation are also determined from the solution of the spectral problem.

Because of the complexity of determining these quantities, in particular, matrix elements $H_{\boldsymbol{k},\boldsymbol{k}_1}$, simplified equations were derived on the basis of the asymptotic analysis of the spectral problem for the Orr–Sommerfeld equation for $\alpha\mathrm{Re} \to \infty$ (α is the streamwise wavenumber and Re is the Reynolds number).

Below we give the results of numerical calculation of the spectral characteristics for the Blasius profile and for a self-similar turbulent profile [9, 10], which are necessary to justify the approaches of [6–8].

1. Formulation of the Problem. The authors of [6–8] considered some possibilities of the nonlinear description of the flow in the laminar and turbulent regions of the boundary layer on a flat plate using flow-field decomposition into a series in eigenfunctions of the Orr–Sommerfeld equation. In the general case, one also has to consider the Squire equation, since the Navier–Stokes equations for the fields of velocity u, v, w and pressure p may be represented in the form of a system of Orr–Sommerfeld and Squire equations relative to the vertical components of velocity v and vorticity η with nonlinear right parts [5]. The linear parts of the equations with the boundary conditions $\hat{v} = d\hat{v}/dy = \hat{\eta} = 0$, $y = 0$, and $y = \infty$ yield the known spectral problems [5]. The quantities marked by the hat symbol are the Fourier transforms of the initial quantities:

$$f = \int\limits_{-\infty}^{\infty} d\alpha \int\limits_{-\infty}^{\infty} d\beta \int\limits_{-\infty}^{\infty} d\omega \hat{f}(y) \exp(i\alpha x + i\beta z - i\omega t), \qquad \omega = \alpha c.$$

Here $k^2 = \alpha^2 + \beta^2$, β is the spanwise wavenumber, $\boldsymbol{k} = (\alpha, \beta)$ is the wave vector, and c is the phase velocity. By solving the Orr–Sommerfeld equation, we obtain the eigenvalues (we call them modes) $c_n = c_n(k^2, \alpha\mathrm{Re})$, where $n = 1, 2, 3, \ldots$ is the number of the eigenvalue.

The right part of the Squire equation contains a term proportional to $\hat{v}$; in the absence of this term, we obtain an equation corresponding to the spectrum of eigenvalues (modes) [5]:

$$c_n' = c_n'(k^2, \alpha\mathrm{Re}) = c_n''(\alpha\mathrm{Re}) - i\,\frac{k^2}{\alpha\mathrm{Re}}, \qquad n = 1, 2, 3, \ldots\ .$$

We indicate some conditions of symmetry [5] imposed on the phase velocities $c(k^2, \alpha\mathrm{Re})$ and $c''(\alpha\mathrm{Re})$ and eigenfunctions $\hat{v}(\boldsymbol{k}, \mathrm{Re})$ and $\hat{\eta}(\boldsymbol{k}, \mathrm{Re})$ by the Squire and Orr–Sommerfeld equations and the conditions of reality of the initial physical quantities:

$$c(k^2, \alpha\mathrm{Re}) = c(k^2, -\alpha\mathrm{Re})^*, \quad c''(\alpha\mathrm{Re}) = c''(-\alpha\mathrm{Re})^*, \quad \hat{v}(\boldsymbol{k}) = \hat{v}(-\boldsymbol{k})^*, \quad \hat{\eta}(\boldsymbol{k}) = \hat{\eta}(\boldsymbol{k})^*.$$

The asterisk here denotes complex conjugation. It is convenient to use these conditions for constructing resonance characteristics.

We give the first modes of the Squire and Orr–Sommerfeld equations and also some characteristics determined through them, which refer to resonant interactions of elementary waves, i.e., to the resonance of the Squire and Orr–Sommerfeld modes,

$$c_n(k^2, \alpha\mathrm{Re}) = c_m'(k^2, \alpha\mathrm{Re}), \qquad m,\, n = 1,\, 2,\, 3, \ldots\ , \tag{1.1}$$

and to the three-wave resonance of Orr–Sommerfeld modes

$$\mathrm{Real}\,[\omega_l(\boldsymbol{k})] = \mathrm{Real}\,[\omega_m(\boldsymbol{k}_1)] + \mathrm{Real}\,[\omega_n(\boldsymbol{k}_2)] \quad (l,\, m,\, n = 1,\, 2,\, 3, \ldots; \quad \boldsymbol{k} = \boldsymbol{k}_1 + \boldsymbol{k}_2),$$

where $\omega_l(\boldsymbol{k}) = \alpha c_l(k^2, \alpha\mathrm{Re})$.

Similar characteristics were found in many papers (see, for example, [5, 11, 12]); however, it is necessary to find them again to perform special processing that would allow one to confirm or reject the assumptions of [6–8] with a good degree of accuracy.

The numerical method of solving the spectral problems at this stage was as follows: a semi-infinite domain $[0; \infty)$ was replaced by a finite domain $[0; 10]$, and a grid (201×351 points) was introduced in which the initial equations were represented in the difference form (by integration from one half-node to another) with the second order of accuracy.

For $y \geqslant 10$, the eigenfunction of the Squire equation was assumed to be equal to $q\exp(-\lambda y)$, where $\lambda = -(i\alpha\,\mathrm{Re}\,(1-c))^{1/2}$, whence it follows the boundary condition [11] $\hat{\eta}'(10) + \lambda\hat{\eta}(10) = 0$. Similarly, for the Orr–Sommerfeld equation in this region we assume that

$$\hat{v} = q_1 \exp(-\lambda_1 y) + q_2 \exp(-\lambda_2 y), \tag{1.2}$$

where $\lambda_1 = k$ and $\lambda_2 = (k^2 + i\alpha\,\mathrm{Re}(1-c))^{1/2}$. From relation (1.2) and its first three derivatives we obtain the following boundary conditions [11]:

$$\hat{v}'' + (\lambda_1 + \lambda_2)\hat{v}' + \lambda_1\lambda_2\hat{v} = 0, \qquad \hat{v}''' + (\lambda_1 + \lambda_2)\hat{v}'' + \lambda_1\lambda_2\hat{v}' = 0. \tag{1.3}$$

The problem with the boundary conditions (1.3) reduces to the solution of the ordinary spectral problem for a doubled number of variables (see, for example, [11]).

However, if the value of $|\alpha\,\mathrm{Re}(1-c)|$ is rather high, we may use the boundary condition $\hat{\eta}(10) = 0$ for the Squire equation and ignore the second term in the right part of formula (1.2) for the Orr–Sommerfeld equation. Then we can obtain simplified boundary conditions

$$\hat{v}' + k\hat{v} = 0, \qquad \hat{v}'' + k\hat{v}' = 0,$$

which do not include the phase velocity c, which allows a twofold reduction of the dimension of the problem.

The eigenvalues of the spectral problem described above for a given velocity profile were found using standard programs for solving the generalized spectral problem. The accuracy of results was evaluated by comparison with the data of [12].

2. Laminar Boundary Layer. The Blasius profile was considered as the velocity profile of the main flow.

The Squire equation. In this equation, spectrum of phase velocities $c'_n(k^2, \alpha\,\mathrm{Re})$ $(n = 1, 2, 3, \ldots)$, which depends on α and β, can be reduced by a simple substitution to the spectrum $c''_n(\alpha\,\mathrm{Re}) = c'_n(k^2, \alpha\,\mathrm{Re}) + ik^2/(\alpha\,\mathrm{Re})$, which depends only on $\alpha\mathrm{Re}$. Thus, the problem is significantly simplified. The asymptotic solution $c''(\alpha\mathrm{Re})$ for the parameter $\alpha\mathrm{Re}$ for $\alpha\mathrm{Re} \gg 1$ can be easily obtained:

$$c''_j(\alpha\mathrm{Re}) = -\delta\lambda_j p + O(\delta^2), \qquad p = U'(0)/2 \approx 44/265, \qquad \delta = (ip\alpha\mathrm{Re})^{-1/3},$$

$$\mathrm{Ai}\,(\lambda_j) = 0, \qquad \lambda_1 \approx -2,338\,11 \qquad (j = 1, 2, \ldots).$$

Here $\mathrm{Ai}\,(x)$ is the Airy function and j is the mode number. It should be noted that the Squire modes depend monotonically on the mode number.

Using this asymptotic solution, we obtained the formula $c''_n(\alpha\mathrm{Re}) = A_n/(\alpha\mathrm{Re})^{1/3} + B_n/(\alpha\mathrm{Re})^{2/3}$, which yields the calculation results for $\alpha\mathrm{Re}/500 \in [0.001; 3]$ and ensures approximation for large values of $\alpha\mathrm{Re}$.

The calculation results were used to study the resonance of the Squire modes and unstable Orr–Sommerfeld mode.

The Orr–Sommerfeld Equation. This equation was solved for the Blasius profile within the range of Reynolds numbers from 500 to 3000 for $\alpha \in [0.005; 1.8]$ and $\beta \in [0; 1.8]$.

TABLE 1

Re	a	b	$\varepsilon^2 d$
500	0.24610402	0.96970043	−0.00256494
1000	0.21921957	0.94623006	−0.00177655
1500	0.20552628	0.91792750	−0.00145604
2000	0.19858133	0.88027801	−0.00122656
3000	0.19144657	0.85439075	−0.00100397

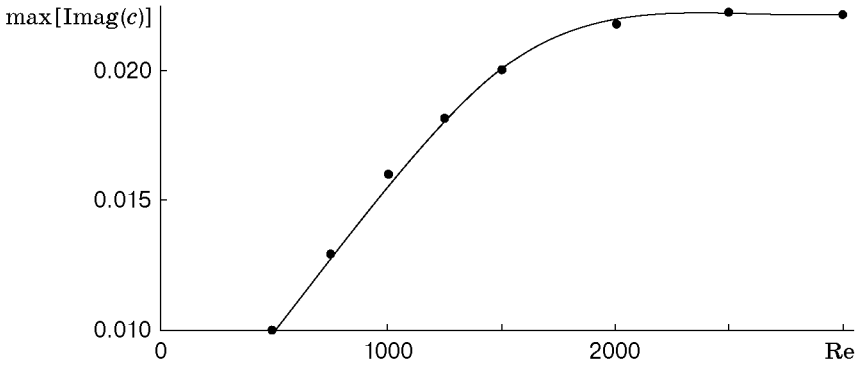

Fig. 1

Zharov [6] proposed an approximation of the phase velocity near the origin:

$$c(\boldsymbol{k}) = a(\mathrm{Re}) + b(\mathrm{Re})k + i\varepsilon^2 d(\mathrm{Re})/\alpha,$$

where $\mathrm{Re} = \mathrm{Re}(\bar{X}_0)$ is the Reynolds number based on the momentum thickness. The values of the coefficients a, b, and d are listed in Table 1.

This approximation is valid within the range $\alpha \in [0.005; 0.14]$. In addition, in the region $\alpha \in [0.005; 1.8]$ and $\beta \in [0; 1.8]$, the phase velocities were represented using the piecewise-polynomial interpolation with respect to α and β. In this form, the data were used to study the resonances. Gol'dshtik and Shtern [11] derived a dependence of the phase velocity in a wide range of α (up to $\alpha \approx 10^3$) for $\beta = 0$. The results of the present work together with the asymptotic solution for $k \gg 1$ obtained in [7] are in good agreement with the results of [11].

Figure 1 shows the dependence of the maximum growth rate of TS waves on the Reynolds number (points are the calculation results). An increase in the growth rate with its subsequent stabilization is observed in the interval Re = 500–3000. The region of instability in the coordinates α, β is pressed toward the origin and extended along the β axis.

The dashed curves in Fig. 2 show the level of Real $[c(\alpha, \beta)]$ for Re = 500. We note that, near the origin, they are close to circumferences whose centers are on the α axis. A similar behavior of the curves near the origin is observed within the entire range of Reynolds numbers under study.

To describe the weakly nonlinear dynamics of the wave packet in a laminar boundary layer, Zharov [6] proposed an approximation where the vertical components of the velocity of oscillations and vorticity were decomposed into a series in terms of eigenfunctions of the Orr–Sommerfeld and Squire equations, respectively, and only the first modes with the least decay were taken into account. It turned out that the coefficient at the first eigenfunction of the Squire equation (it can be easily written explicitly) contains the difference $c - c'$ in the denominator. It is important in using this approximation that this difference does not vanish. The resonance of the lowest Squire and TS waves was studied; the results are plotted in Fig. 3, which shows the solutions of the equations Real $[c - c'] = 0$ and Imag $[c - c'] = 0$ for the unstable TS mode and the first Squire mode. In the region of wavenumbers considered, there is no solution for the Squire modes of higher order. A similar pattern is observed within the entire range of Reynolds numbers examined. Since the curves in Fig. 3 do not intersect, system (1.1) has no solution. Hence, the resonance considered is absent for $\alpha \in [0.005; 1.8]$ and $\beta \in [0; 1.8]$.

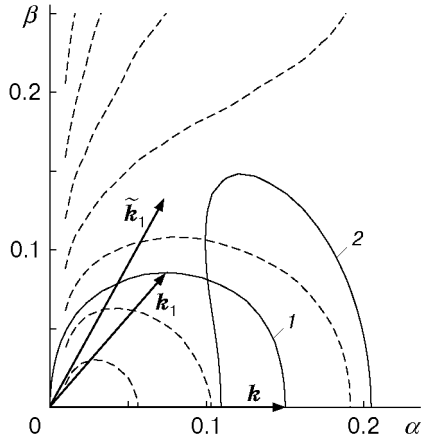

Fig. 2

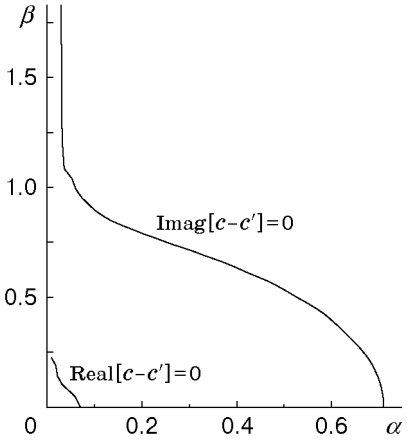

Fig. 3

The solid curves in Fig. 2 show the three-wave resonance of TS waves (curve 1) and the boundary of the amplification region (curve 2) for Re = 500. The vector $\boldsymbol{k}$ corresponds to the maximum growth rate; the vectors $\tilde{\boldsymbol{k}}_1$ and $\boldsymbol{k}_1$ are the subharmonics for the following cases, respectively: (1) asymptotic limit for $\mathrm{Re} \to \infty$ [7]; (2) asymptotic limit for Re = 500. In the first case, the slope of the harmonic with the frequency $\omega(0.155; 0)/2$ is 60°; in the second case, it is approximately 50° (the end of the vector $\boldsymbol{k}_1$ lies on curve 1 of three-wave resonances). A similar structure of the three-wave resonance is observed for other values of Re within the region examined. We note that the slope of subharmonics for all Re is approximately 50°.

The value of $H_{0,0}$ was found as the limit $H_{\boldsymbol{k},\,\boldsymbol{k}\,-\,\boldsymbol{k}_1}$, where the vector $\boldsymbol{k}$ is directed along the longitudinal axis of the space of wavenumbers, and $\boldsymbol{k}_1$ and $\boldsymbol{k} - \boldsymbol{k}_1$ are its subharmonics for $\boldsymbol{k} \to 0$. It turned out that $\mathrm{Real}\,[H_{\boldsymbol{k},\,\boldsymbol{k}\,-\,\boldsymbol{k}_1}]$ and $\mathrm{Imag}\,[H_{\boldsymbol{k},\,\boldsymbol{k}\,-\,\boldsymbol{k}_1}]$ are the power functions $\alpha^{0.72}$ and $\alpha^{0.45}$, respectively, as $\alpha \to 0$. By renormalization of the initial equations, one can make the new quantity $H_{0,0}$ finite and real, which regularizes the model equations obtained in [6].

3. Turbulent Boundary Layer. In studying the turbulent boundary layer, we used the velocity profile obtained in [10] by generalization of theoretical and empirical data:

$$\frac{u}{u_*} = 5.424 \arctan\Big(\frac{2y/\delta_\nu - 8.15}{16.7}\Big) + \log\Big(\frac{(y/\delta_\nu + 10.6)^{9.6}}{(y/\delta_\nu)^2 - 8.15y/\delta_\nu + 86}\Big) - 3.52$$
$$+ 2.44\Big[\Pi\Big(6\Big(\frac{y}{\delta}\Big)^2 - 4\Big(\frac{y}{\delta}\Big)^3\Big) + \Big(\frac{y}{\delta}\Big)^2\Big(1 - \frac{y}{\delta}\Big)\Big]. \qquad (3.1)$$

Here $u_* = (\tau_w/\rho)^{1/2}$ is the dynamic velocity, $\Pi = 0.14$, $\delta_\nu = \nu/u_*$, and δ is the boundary-layer thickness. The relation between δ_ν and δ is set by the formula $\delta_\nu/\delta = (c_f/2)^{-1/2}\,\mathrm{Re}$, where Re is the Reynolds number based on the boundary-layer thickness δ, $u(\delta) = 0.99u_\infty$, and the friction coefficient c_f is determined from the equation $c_f^{-1/2} = 1.77 \ln(\mathrm{Re}\, c_f/0.33) + 2.4$ [9].

It follows from formula (3.1) that the turbulent velocity profile has two scales. We note that the second derivative of profile (3.1) is nonmonotonic for $y/\delta \to 1$. Hence, the known approximations of the available experimental data do not model all the properties of the velocity profile in the turbulent boundary layer.

Profile (3.1) was compared with the experimental data of [3]. Some difference was observed in the region of action of the wall law, but the experimental profile and profile (3.1) coincided if the ratio of the Reynolds numbers obtained in [3, 10] was roughly equal to 1.42.

Squire Equation. The spectral problem for the Squire equation was solved using the methods described above. The modes were chosen taking into account the form of eigenfunctions. The solid curves in Figs. 4 and 5 show the real and imaginary parts of the phase velocity of the Squire modes for Re = 500 (the numbers near the curves correspond to the mode number j). The real part of the phase velocity for different modes is a system of nonintersecting curves; the curves corresponding to a greater mode number are higher than the curves corresponding to a lower number. This is not true for the curves that describe the imaginary part. The data obtained here are used for seeking possible rigorous resonances with TS waves.

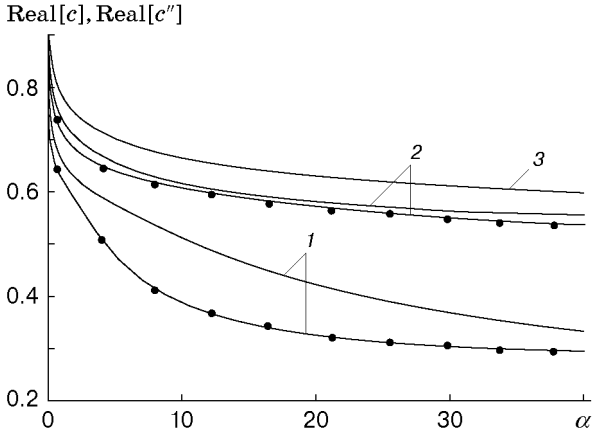

Fig. 4

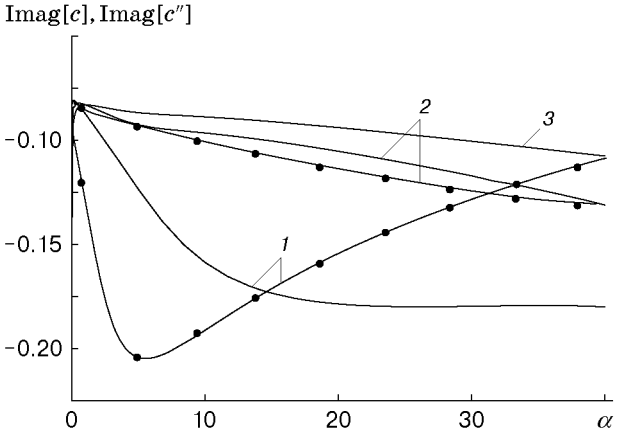

Fig. 5

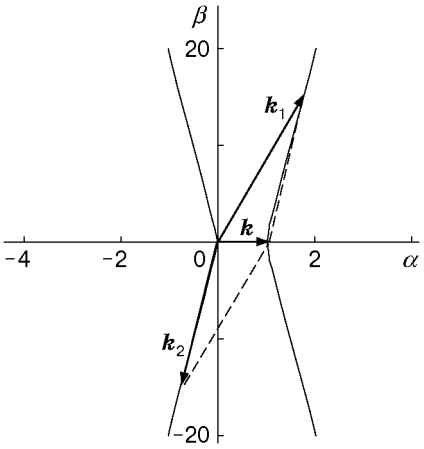

Fig. 6

Orr–Sommerfeld Equation. The phase velocities for TS wave modes were sought in the interval $\alpha \in [0.05; 40]$ and $\beta \in [0; 30]$. To illustrate the behavior of dispersion dependences in Figs. 4 and 5, the points mark the curves that describe the behavior of the real and imaginary parts of the phase velocities of the two lowest modes of TS waves $c(\alpha, 0)$ as a function of α for $\beta = 0$. As in the laminar case, there is no resonance of the Squire and TS wave modes within the range of wavenumbers examined.

Figure 6 shows the three-wave resonance of the lowest TS wave mode (judging by the real part of the phase velocity). The curves that characterize this resonance are significantly different from the three-wave resonance on the Blasius profile.

4. Discussion of Results. It follows from the results obtained that there is no rigorous resonance of the Squire and TS wave modes within the range of wavenumbers considered both in laminar and turbulent boundary layers.

The data on dispersion dependences show that the assumptions accepted in [6] for deriving simplified equations that describe the weakly nonlinear dynamics of wave packets are valid for TS waves of the lowest mode of the Orr–Sommerfeld equations in a laminar boundary layer. These assumptions include the isotropy of Real $[c(\alpha, \beta)]$ relative to the parameters α and β (see Fig. 2), the linear dependence on k in a certain small neighborhood of zero, and the finiteness of Imag $[\omega]$ for $k \to 0$ (see Table 1).

Some properties of the three-wave resonance are common for the spatial and temporal formulations of the problem, which allows us to compare the results obtained in experiments with a vibrating strip. Thus, the three-wave resonance curve (curve 2 in Fig. 2) explains the appearance of a continuous spectrum found in the experimental study of this phenomenon in [1]; the reason is that the three-wave resonance with the

wave vector $\boldsymbol{k}$ encompasses simultaneously all pairs of waves with the ends of wave vectors on curve 2, and their sum is equal to the vector $\boldsymbol{k}$. The frequency of waves that come into resonance changes continuously from 0 to $\omega(\boldsymbol{k})$ (the dynamics of amplitudes should obey the integrodifferential equation). In addition, the slope of the wave vector of the subharmonic to the longitudinal axis is estimated in [1] to be within the range of 45–59° for the Reynolds number changing from the first critical value to a value corresponding to the transition point. The value of 50° obtained on the Blasius profile in the present work is within this interval.

In a turbulent boundary layer (Re $\approx$ 40,000), unstable modes of TS waves were not found, in contrast to [13]. In the examined range of wave vectors, the existence of a three-wave resonance was noted, whose curves (see Fig. 6) may be interpreted as follows. If some inhomogeneity ($\boldsymbol{k}$, $\boldsymbol{k}_1$), two-dimensional with respect to x and z, appears in the flow, it may come into resonance (since it can be represented as a Fourier integral in planar and oblique waves) with TS waves whose wave vector $\boldsymbol{k}_2$ is almost perpendicular to the flow direction. Similar to Görtler waves, these waves form a spanwise structure observed at the bottom of the turbulent boundary layer [3]. In this case, the structure may be related to the presence of an inhomogeneity, which is a localized region of circulation flow near the wall. An analysis of the laminar part of the boundary layer shows that these inhomogeneities may arise because of the nonlinear dynamics of localized perturbations [2, 4, 7, 14].

Thus, from the physical viewpoint, the presence of the three-wave resonance may explain the appearance of a spanwise structure similar to Görtler vortices. (The possible relation of the three-wave resonance with streamwise structures in a turbulent boundary layer was noted in [11], though the mechanism of formation of streamwise structures is not described in that paper.) The method of identification of this (unsteady) structure in a turbulent boundary layer described in [7, 8] is similar to the method of identification of a coherent structure in a laminar boundary layer considered in [6]. These structures are similar to those described in [4] with the only difference being that the structures considered in the present work are unsteady.

This work was supported by the Russian Foundation for Fundamental Research (Grant No. 99-01-01239) and the State Program for Supporting Leading Scientific Schools (Grant No. 96-15-96063).

REFERENCES

1. Y. S. Kachanov, "Physical mechanisms of laminar–boundary–layer transition," *Annu. Rev. Fluid Mech.*, **26**, 411–482 (1994).
2. E. U. Repik and Yu. P. Sosedko, "Investigation of the intermittent flow structure in the near-wall region of a turbulent boundary layer," in: *Turbulent Flows* (collected scientific papers) [in Russian], Nauka, Moscow (1974), pp. 172–184.
3. S. K. Robinson, "Coherent motions in the turbulent boundary layer," *Annu. Rev. Fluid Mech.*, **23**, 601–639 (1991).
4. A. V. Boiko, G. R. Grek, A. V. Dovgal', and V. V. Kozlov, *Origination of Turbulence in Near-Wall Flows* [in Russian], Nauka, Novosibirsk (1999).
5. D. J. Benney and H. L. Gustavsson, "A new mechanism for linear and nonlinear hydrodynamic instability," *Stud. Appl. Math.*, **64**, 185–209 (1981).
6. V. A. Zharov, "Variant of description of the weakly nonlinear dynamics of the wave packet in the boundary layer on a flat plate in an incompressible fluid," *Tr. TsAGI*, No. 2523 (1993).
7. V. A. Zharov, "Wave theory of a developed turbulent boundary layer," *Uch. Zap. TsAGI*, **17**, No. 5, 28–38 (1986).
8. S. L. Gorelov, V. A. Zharov, and Y. I. Khlopkov, "The kinetic approaches to the turbulence description," in: *Rarefied Gas Dynamics*, Proc. of the 20th Int. Symp. (Beijing, China, August 19–23, 1996), Peking Univ. Press, Beijing (1997).
9. V. A. Kader and A. M. Yaglom, "Laws of similarity for near-wall turbulent flows," VINITI, Moscow (1980), pp. 81–155. (*Itogi Nauki Tekh., Ser. Mekh. Zhidk. Gaza*, **15**.)
10. A. J. Musker, "Explicit expression for the smooth velocity distribution in turbulent boundary layer," *AIAA J.*, **17**, No. 6, 655–657 (1979).

11. M. A. Gol'dshtik and V. N. Shtern, *Hydrodynamic Stability and Turbulence* [in Russian], Nauka, Novosibirsk (1977).
12. L. M. Mack, "A numerical study of the temporal eigenvalues spectrum of the Blasius boundary layer," *J. Fluid Mech.*, **73**, 497–520 (1976).
13. T. Sadatoshi, "Visual observation on the amplification of artificial disturbances in turbulent shear flows," *Phys. Fluids*, **26**, No. 10, 2801–2806 (1983).
14. V. S. Sadovskii, N. P. Sinitsyna, and G. I. Taganov, "Numerical study of the mathematical model of the near-wall flow in a turbulent boundary layer," in: *Near-Wall Turbulent Flow* [in Russian], Part 1, Nauka, Novosibirsk (1975), pp. 94–116.